

cpth-s4540696
 Crete-96-11
 hep-ph/9606348

ON SPHERICALLY-SYMMETRIC SOLUTIONS IN THE TWO-HIGGS STANDARD MODEL

C. Bachas ♠, P. Tinyakov ◇ and T.N. Tomaras ♣

♦ Centre de Physique Théorique, Ecole Polytechnique, 91128 Palaiseau,
 FRANCE
 email: *bachas@orphee.polytechnique.fr*

◇ Institute for Nuclear Research, 60th October Anniversary prospect 7a,
 117 312 Moscow, RUSSIA
 email: *tinyakov@ms2.inr.ac.ru*

♣ Dept. of Physics and Institute of Plasma Physics, University of Crete,
 and Research Center of Crete,
 P.O. Box 2208, 710 03 Heraklion, GREECE
 email: *tomaras@physics.uch.gr*

ABSTRACT

We report the results of a numerical search for non-topological solitons in the two-Higgs standard model, characterized by the non-trivial winding, $\pi_3(S^3)$, of the relative phase of the two doublets. In a region of (weak-coupling) parameter space we identify a branch of winding solutions, which are lower in energy than the embedded standard sphaleron and deformed (bi)sphalerons. Contrary, however, to what happens in 2d toy models, these solutions remain unstable even for very large Higgs masses.

Two of us have analyzed recently non-topological winding solitons in renormalizable gauge models with two Higgs scalars. Such solitons arise in two and three space-time dimensions [1], and can be embedded as extended membrane defects in the weakly-coupled two-Higgs standard model (2HSM) [2]. It was furthermore argued by analogy [1] that the 2HSM may have string-like or particle-like excitations characterized by a non-trivial mapping of the spatial three sphere onto the relative phase of the two doublets. Depending on the details of the potential, the relevant quantity could be either the Hopf invariant, $\pi_3(S^2)$, or the winding number, $\pi_3(S^3)$. Here we report the results of a numerical search for solitons of the latter type. The search revealed indeed a branch of winding solutions, but unlike their 2d analogs these stay classically unstable for arbitrarily large Higgs masses. These new solutions could nevertheless be of interest for the study of electroweak baryogenesis in the 2HSM [3]. Sphaleron solutions in the 2HSM have been discussed previously in ref. [4] and in a different context in ref. [5].

There exists a close analogy between sphaleron solutions in the minimal standard model [6, 7, 8], and those in the abelian-Higgs [10] or global double-well [9] models on the circle. Similarly, the structure of classical solutions in the 2HSM is strongly reminiscent of that in the abelian two-Higgs, or in the global mexican-hat model on the circle. This latter model is defined by the action

$$S = \int dt \int_0^{2\pi L} dx \left[\frac{1}{2} \partial_\mu \Phi^* \partial^\mu \Phi - \frac{\lambda}{4} (\Phi^* \Phi - v^2)^2 \right], \quad (1)$$

whose single classically-relevant parameter is $mL = \sqrt{2\lambda}vL$. We henceforth set $L = 1$. Static solutions correspond to motions of a particle in the inverted mexican-hat potential with period 2π . One solution, which exists for all values of m and can be thought of as the basic sphaleron ^{*}, corresponds to the particle sitting at the bottom of the inverted hat. It has energy $\pi m^4/8\lambda$, starts out with two negative modes, and acquires two extra ones every time $m/\sqrt{2}$ crosses a positive integer n . Two extra branches of solutions bifurcate

^{*}Though it does not in this case represent a minimum-height passage between two discrete degenerate vacua.

at these points: the S_n branch describes an n -fold oscillation about the bottom of the inverted hat, with zero angular momentum. These solutions, also present in the double-well model, are everywhere unstable and are the analogs of the deformed sphalerons of the standard model [9, 7]. The W_n branches on the other hand describe an n -fold rotation around the tip of the hat, and have no analog in the one-Higgs model. The solutions have a constant scalar magnitude $\Phi^* \Phi = (m^2 - 2n^2)/2\lambda$, an energy equal to $\pi n^2(m^2 - n^2)/2\lambda$, and become classically stable beyond the critical values $m^2 = 6n^2 - 1$ [1]. New branches, \tilde{W}_n , emerge at these points; they have slightly higher energy and correspond to winding motions with an oscillating scalar magnitude. Further bifurcations occur along the $W_{n>1}$ branches, and possibly also along S_n and \tilde{W}_n , but an exhaustive analysis is beyond the scope of this letter. Figure 1 is an illustration of the topological tree of solutions. The main lesson to retain

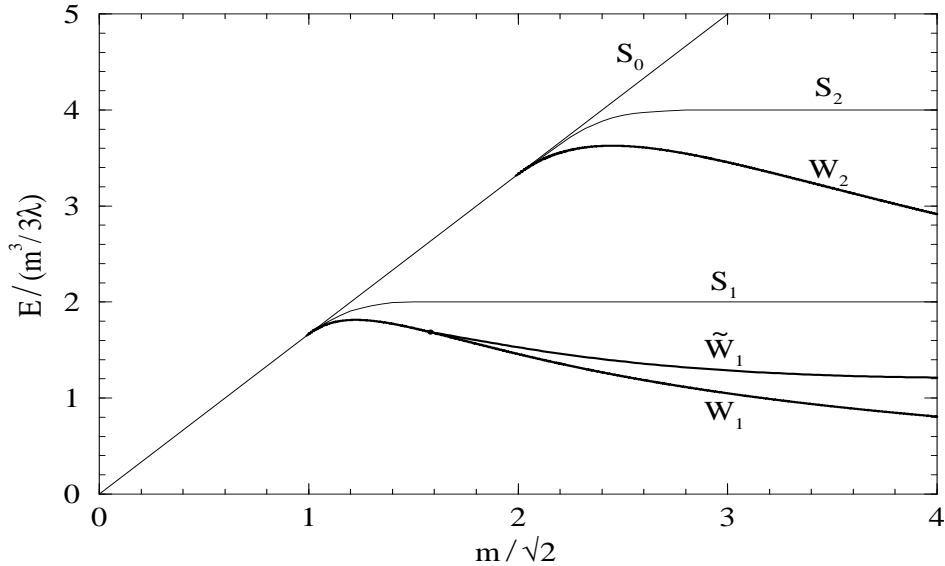


Figure 1. Part of the tree of classical solutions for the model (1). The vertical axis gives the energy, measured in units of $m^3/3\lambda$ so as to simplify comparison with ref. [9]. The \tilde{W}_1 branch is drawn out of scale: its energy differs by only $\sim 1\%$ from the energy of W_1 .

from this toy model is that for $m > \sqrt{2}$ the winding solution on the W_1 branch is the one with lowest energy, and that furthermore for $m > \sqrt{5}$ it becomes a classically-stable soliton.

Using this toy model as a guide, we turn now to the 2HSM. We will work with the simplifying assumptions of vanishing Weinberg angle and of a potential consisting of two independent mexican hats. We believe that these restrictions are optimal, in the sense of favouring the stability of the sought-for winding solutions. We also restricted our search to spherically-symmetric configurations. The action is

$$S = \frac{1}{g^2} \int d^4x \left[-\frac{1}{2} Tr(W_{\mu\nu}W^{\mu\nu}) + \sum_{a=1,2} (D_\mu H_a)^\dagger (D^\mu H_a) - \sum_{a=1,2} \frac{\lambda_a}{g^2} (H_a^\dagger H_a - g^2 v_a^2)^2 \right] \quad (2)$$

with $D_\mu H_a = (\partial_\mu + W_\mu)H_a$, for $a = 1, 2$, and $W_{\mu\nu} = [D_\mu, D_\nu]$. We fix the length scale by setting $m_W = g\sqrt{(v_1^2 + v_2^2)/2} = 1$, and scale out of the action the semiclassical parameter $\alpha_W = g^2/4\pi$. There remain three classically-relevant parameters: the two radial Higgs masses $m_a = 2\sqrt{\lambda_a}v_a$, and $\tan\beta = v_2/v_1$.

The general spherically-symmetric static ansatz, following the conventions of Yaffe [8], reads

$$\begin{aligned} W_0 &= w_0 \tau_i n_i / 2i, \\ W_i &= \frac{1}{2i} \left[(a-1) \epsilon_{ijk} \tau_j n_k / r + b (\delta_{ij} - n_i n_j) \tau_j / r + w_1 n_i n_j \tau_j \right] \\ H_a &= (\mu_a + i \nu_a n_i \tau_i) \xi \end{aligned} \quad (3)$$

where n_i is the unit vector in the direction of \mathbf{r} , τ_i are the three Pauli matrices, ξ is a constant unit doublet and $w_0, w_1, a, b, \mu_a, \nu_a$ are functions of r to be determined by the stationarity of the energy. It is convenient to choose the gauge $w_0 = 0$, and then solve Gauss' constraint to obtain $w_1 = 0$ [8]. Defining the complex fields $\phi_a = \mu_a + i \nu_a \equiv f_a \exp(i\theta_a)$ ($a = 1, 2$) and

$\chi = a + ib = |\chi| \exp(i\psi)$, one can put the energy functional in the form:

$$E = \frac{1}{\alpha_W} \int_0^\infty dr \left\{ |\chi'|^2 + 2r^2 \cos^2 \beta (|\phi_1'|^2 + |\phi_2'|^2) + \frac{1}{2r^2} (|\chi|^2 - 1)^2 + \cos^2 \beta (|\chi|^2 + 1) (|\phi_1|^2 + |\phi_2|^2) - 2 \cos^2 \beta \operatorname{Re}[\chi^* (\phi_1^2 + \phi_2^2)] + \frac{1}{2} m_1^2 r^2 \cos^2 \beta (|\phi_1|^2 - 1)^2 + \frac{1}{2} m_2^2 r^2 \frac{\cos^2 \beta}{\tan^2 \beta} (|\phi_2|^2 - \tan^2 \beta)^2 \right\}, \quad (4)$$

with primes standing for derivatives with respect to r . The above expression is invariant under a simultaneous rotation of ϕ_1 , ϕ_2 and χ by a phase ω, ω and 2ω respectively, as well as under independent changes of sign of ϕ_1 and ϕ_2 . These symmetries together with the requirement of finite energy allows us to fix the boundary conditions at $r = \infty$ in the form:

$$\chi \rightarrow 1, \phi_1 \rightarrow 1 \text{ and } \phi_2 \rightarrow \tan \beta. \quad (5)$$

At $r = 0$ on the other hand, finiteness of the energy, of the gauge current and of the field strength imply [8]:

$$|\chi| \rightarrow 1, \chi^* \phi_a^2 \rightarrow |\phi_a|^2 \text{ and } \chi' \rightarrow 0. \quad (6)$$

Notice in particular that at the origin either $f_a = 0$, or else $2\theta_a - \psi = 0 \pmod{2\pi}$. For configurations with non-vanishing Higgs magnitudes we may conclude that

$$\theta_1 - \theta_2 \Big|_{r=0} = N\pi \quad (7)$$

The integer N is the gauge-invariant winding number characterizing the mapping from the spatial S^3 onto the $SU(2)$ manifold of the relative phase of the two doublets [1].

We used the relaxation method [11] to integrate the field equations numerically. Starting with some initial guess $\{\hat{\Phi}\}$ for the solution, one linearizes the static field equations, solves them, and adds the result to $\{\hat{\Phi}\}$ thus obtaining an improved guess for the next iteration. The radial coordinate r was replaced by $n+1=201$ points r_i , with $r_0 = 0$ and $r_n = R = 20$. This was sufficient to achieve an accuracy of order 10^{-3} to 10^{-4} in the energy of the

solutions. Following ref. [8] we distributed the lattice points according to the formula $r_k = (1 - e^{ks/n})/(e^{ks/n} - \mu)$, with $s = \ln[(1 + \mu R)/(1 + R)]$ and $\mu = \max(m_1, m_2)$. The linearized equations at each iteration step take the form $E_{IJ}^{(2)} \delta\Phi^J = E_I^{(1)}$ where $\delta\Phi$ is a vector of dimension $n \times (\#\text{fields}) = 1200$, normalized so that the kinetic energy reads $\frac{1}{2} \sum \delta\dot{\Phi}^i \delta\dot{\Phi}^i$, and $E^{(1)}, E^{(2)}$ are respectively the first and second variations of the static energy, eq. (4). The matrix $E^{(2)}$ has a special block-three-diagonal form, each block corresponding to the six fields at the same lattice point. We have exploited this special form to invert the matrix by a forward-elimination and back-substitution procedure. This same procedure also allowed us to calculate the spectrum of negative fluctuation modes around the solutions.

Figure 2 summarizes schematically the tree of solutions that we have found in the particular case of equal Higgs masses, $m_1 = m_2 \equiv m$. This further restriction of parameter space has the following convenient feature: any solution $\{\hat{H}, \hat{W}_\mu\}$, of the one-doublet model with Higgs mass m and $m_W = 1$, yields a solution $\{H_1 = \hat{H}\cos\beta, H_2 = \hat{H}\sin\beta, W_\mu = \hat{W}_\mu\}$ of the 2HSM with the same total energy though a different fluctuation spectrum. The branches S_0 and S_1 in particular correspond to the standard sphaleron [6] and deformed (bi)sphalerons [7, 8] of the minimal model, and have been used to check the accuracy of our numerical routines. All other branches shown in figure 2 have no analog in the one-doublet model.

The standard sphaleron (with χ, ϕ_a real) is the only solution we have found for $m/m_W \leq 5.5$. It has a single mode of instability in this range, but develops a second one where the new branches of winding solutions, (W_1) and its conjugate, bifurcate. Extra negative modes appear at each subsequent bifurcation: at $m/m_W \simeq 12$ (first deformed sphalerons), at $m/m_W \simeq 50$ (doubly-winding solutions), at $m/m_W \simeq 138$ (second deformed sphalerons) and so on down the line. This sequence of bifurcations is strongly reminiscent of the 2d toy model, except that the W_n and S_n branches do not emerge in this case simultaneously. Notice that the topological invariant, $\sum_{\text{solutions}} (-)^{n_s}$,

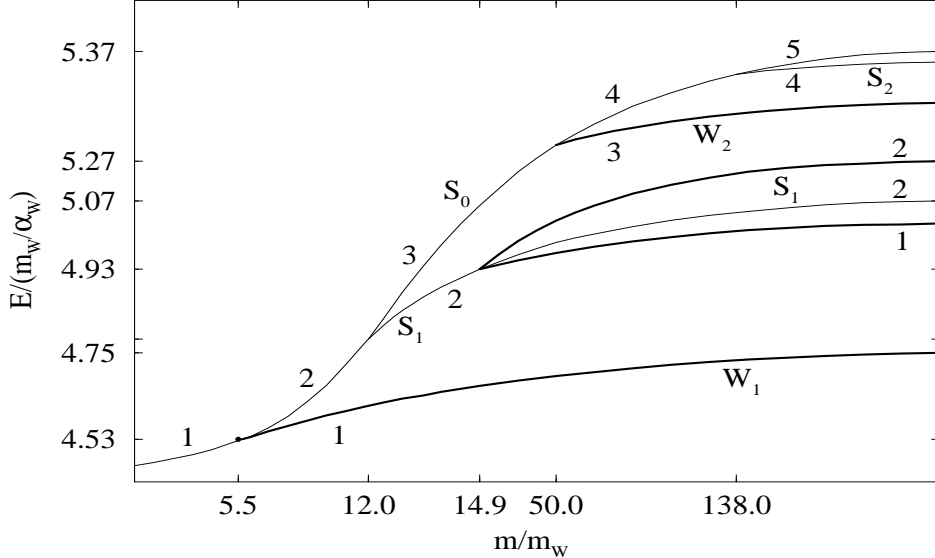


Figure 2. Solutions of the two-Higgs model, eq. (2), for $\tan\beta=1$, as function of the (common) radial Higgs mass m . Both the vertical and the horizontal axes have non-uniform scales. The number of negative modes is shown explicitly for every branch. The winding branch, W_1 , emerges out of the main sphaleron at $m/m_W \simeq 5.5$, but remains unstable at least up to a mass ratio of ~ 200 .

with n_s the number of unstable modes of the solution, is conserved at all bifurcation points. This is also true at $m/m_W \simeq 14.9$, where a once- and a twice-unstable branch emerge out of the first deformed sphaleron, corresponding to the transformation of a local maximum, into two maxima separated by a lower-energy saddle.

The most interesting feature of Figure 2 is of course the winding branch W_1 , which on the basis of the 2d analog could have evolved into a stable soliton at sufficiently large Higgs masses. The negative eigenvalue does not, however, cross the zero axis in this case, at least all the way out to $m/m_W \sim 200$ (see table 1) [†]. By performing a numerical scan, we have checked that

[†] Such large values of parameters are in any case academic, since the semiclassical approximation cannot be anymore trusted.

the winding branch does not stabilize anywhere inside the larger space of parameters of the potential, eq. (2) (see Table 2). Since we do not expect interactions between the two doublets to improve stability, we believe that such winding solitons do not exist. This is the main conclusion of the present letter.

The unstable solutions are nevertheless of interest in their own right. They emerge inside the region of weak coupling, and can be lower in energy and comparatively less unstable than the known sphaleron and deformed sphaleron solutions, as shown in Table 1. They furthermore continue to exist in a large region of parameter space, which is sampled selectively in table 2. The profile of a typical solution for $\tan\beta = 1.4$, $m_1 = 0.1$ and $m_2 = 10.1$ is plotted in Fig. 3. As is the case with deformed sphalerons in the minimal model, the appearance of the two conjugate W_1 branches corresponds to the splitting of a minimum-height passage in the energy landscape into two. These configurations should thus dominate baryon-number violating transitions at high temperature, in the appropriate regions of parameter space of the 2HSM. More generally, their existence illustrates how rich the configuration space of the 2HSM is. Its exploration could, we believe, reveal many surprising features.

$m_1 = m_2$	E_{W_1}	$-\omega_{W_1}^2$	E_{sph}	$-\omega_{sph}^2$	E_{dsph}	$-\omega_{dsph}^2$
6.0	4.53	5.17	4.53	6.35	—	—
10.0	4.67	3.09	4.78	11.21	—	—
15.0	4.72	2.68	4.95	23.43	4.93	8.44
20.0	4.73	2.55	5.04	42.80	4.99	6.09
30.0	4.74	2.46	5.15	101.1	5.04	5.20
50.0	4.75	2.42	5.25	291.8	5.06	4.97
100.0	4.75	2.41	5.33	1192	5.07	4.75

Table 1. The energy (in units of m_W/α_W) and negative eigenvalue of the fluctuation spectrum (in units of m_W) along the winding branch W_1 , in the symmetric case $\tan\beta=1$ and $m_1=m_2$. We have included for comparison the energy and most negative eigenvalue along the embedded sphaleron and first deformed sphaleron branches, respectively S_0 and S_1 .

m_1	m_2	$\tan\beta$	E_{W_1}	$-\omega_{W_1}^2$
10.0	10.0	0.03	4.78	11.20
10.0	10.0	0.1	4.78	11.14
10.0	10.0	0.5	4.74	5.43
10.0	10.0	1.0	4.67	3.09
10.0	10.0	1.4	4.70	3.70
10.0	10.0	1.8	4.73	4.82
10.0	10.0	2.8	4.76	7.72
10.0	10.0	4.0	4.77	9.83
10.0	10.0	6.0	4.78	10.86
6.0	6.0	2.0	4.53	5.95
5.0	6.0	2.0	4.51	6.05
4.0	6.0	2.0	4.49	5.94
3.0	6.0	2.0	4.46	5.85
2.5	6.0	2.0	4.44	5.80
2.0	6.0	2.0	4.43	5.76
1.5	6.0	2.0	4.40	5.72
10.0	0.0	4.0	3.17	1.42
10.0	0.1	4.0	3.26	1.58
10.0	0.4	4.0	3.45	1.92
10.0	1.0	4.0	3.71	2.45
10.0	2.0	4.0	4.00	3.21
10.0	5.0	4.0	4.45	5.29
10.0	10.0	4.0	4.77	9.83
10.0	15.0	4.0	4.90	6.43
10.0	20.0	4.0	4.95	5.25
10.0	30.0	4.0	4.99	4.67
10.0	40.0	4.0	4.99	4.51

Table 2. The energy and negative eigenvalue of the W_1 branch, for various values of $\tan\beta$ and of the ratio m_2/m_1 . The units are the same as in table 1. Notice that when $\tan\beta\rightarrow 0$ the winding solution merges with the sphaleron. For equal values of the two Higgs masses the lowest-energy, least unstable solution is obtained in the symmetric case $\tan\beta=1$, when the winding is equally shared by the two Higgses.

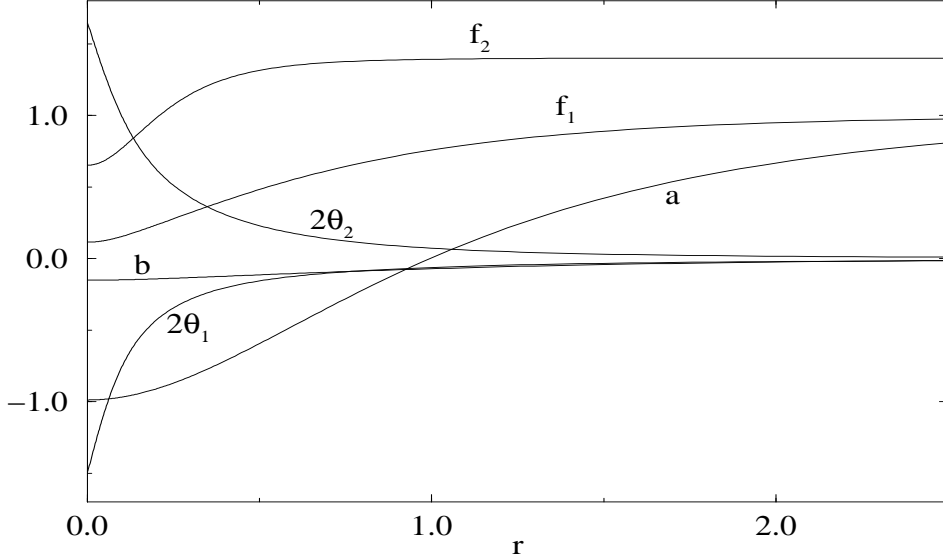


Figure 3. The profile of a solution on the W_1 branch for Higgs masses about 8 and 800 GeV respectively.

Acknowledgments

We acknowledge a useful conversation with Y. Brihaye. C.B. and P.T. thank the Physics Department of the University of Crete and the Research Center of Crete, while P.T. and T.N.T. thank the Centre de Physique Théorique of the Ecole Polytechnique for hospitality, while this work was being completed. The work of C.B and TN.T. was supported in part by the EEC grants CHRX-CT93-0340 and CHRX-CT94-0621, and by the Greek General Secretariat of Research and Technology grant No. 91EΔ358, while that of P.T. by the INTAS grant INTAS-94-2352 and by the Russian Foundation for Fundamental Research, grant 96-02-17804a.

References

- [1] C. Bachas and T.N. Tomaras, Nucl. Phys. **B428** (1994) 209 and Phys. Rev. **D51** (1995) R5356.
- [2] C. Bachas and T.N. Tomaras, Phys. Rev. Lett. **76** (1996) 356.
- [3] V. Kuzmin, V. Rubakov and M. Shaposhnikov, Phys. Lett. **155B** (1985) 36; for recent reviews see N. Turok, in *Perspectives on Higgs Physics*, G. Kane ed., World Scientific 1993, and V.A. Rubakov and M.E. Shaposhnikov, *Electroweak baryon number non-conservation in the early Universe and in high energy collisions*, CERN-TH/96-13, hep-ph/9603208 (to appear in Usp. Fiz. Nauk, v.166, May 1996).
- [4] B. Kastening, R.D. Peccei and X. Zhang, Phys. Lett. **266B** (1991) 413.
- [5] Y. Brihaye, J. Kunz and C. Semay, Phys. Rev. **D42** (1990) 193 and **D44** (1991) 250.
- [6] R. Dashen, B. Hasslacher and A. Neveu, Phys. Rev. **D10** (1974) 4138; N.S. Manton, Phys. Rev. **D28** (1983) 2019; F. Klinkhamer and N.S. Manton, Phys. Rev. **D30** (1984) 2212.
- [7] J. Kunz and Y. Brihaye, Phys. Lett. **216B** (1989) 353.
- [8] L. Yaffe, Phys. Rev. **D40** (1989) 3463.
- [9] N.S. Manton and T.M. Samols, Phys. Lett. **207B** (1988) 179; J.-Q. Liang, H.J.W. Müller-Kirsten and D.H. Tchrakian, Phys. Lett. **282B** (1992) 105.
- [10] Y. Brihaye, S. Giller, P. Kosinski and J. Kunz, Phys. Lett. **293B** (1992) 383.
- [11] W. Press, S. Teukolsky, W. Vetterling and B. Flannery, *Numerical Recipes*, chapter 17. Cambridge University Press 1992.